Modeling of Dynamic Material Behavior in Hot Deformation: Forging of Ti-6242

Y. V. R. K. PRASAD, H. L. GEGEL, S. M. DORAIVELU,
J. C. MALAS, J. T. MORGAN, K. A. LARK, and D. R. BARKER

A new method of modeling material behavior which accounts for the dynamic metallurgical processes occurring during hot deformation is presented. The approach in this method is to consider the workpiece as a dissipator of power in the total processing system and to evaluate the dissipated power co-content $J = \int_0^{\sigma} \dot{\varepsilon} \cdot d\sigma$ from the constitutive equation relating the strain rate ($\dot{\varepsilon}$) to the flow stress (σ). The optimum processing conditions of temperature and strain rate are those corresponding to the maximum or peak in J. It is shown that J is related to the strain-rate sensitivity (m) of the material and reaches a maximum value (J_{max}) when $m = 1$. The efficiency of the power dissipation (J/J_{max}) through metallurgical processes is shown to be an index of the dynamic behavior of the material and is useful in obtaining a unique combination of temperature and strain rate for processing and also in delineating the regions of internal fracture. In this method of modeling, no *a priori* knowledge or evaluation of the atomistic mechanisms is required, and the method is effective even when more than one dissipation process occurs, which is particularly advantageous in the hot processing of commercial alloys having complex microstructures. This method has been applied to modeling of the behavior of Ti-6242 during hot forging. The behavior of $\alpha + \beta$ and β preform microstructures has been examined, and the results show that the optimum condition for hot forging of these preforms is obtained at 927 °C (1200 K) and a strain rate of 10^{-3} s^{-1}. Variations in the efficiency of dissipation with temperature and strain rate are correlated with the dynamic microstructural changes occurring in the material.

I. INTRODUCTION

THE mechanical behavior of materials under processing is generally characterized by constitutive equations which relate the flow stress to the strain, strain rate, and temperature. The constitutive relations are experimentally evaluated using mechanical testing techniques[1] and represented either in the form of empirical rate equations[2] which aid in identification of the specific atomistic rate-controlling mechanisms or in the form of simple algebraic equations[3] which can be used in process modeling. In recent years, hot-forming processes have been successfully modeled using a rigid viscoplastic finite-element method[4,5] which predicts deformation behavior at selected points (nodes) in each element by application of a variational principle. The variational-principle functional ϕ for a rigid viscoplastic material is written as[5]

$$\phi = \int E(\dot{\varepsilon}^*)\, dv - \int \mathbf{F} \cdot \mathbf{V}^* \cdot ds + \tfrac{1}{2} \int K(\dot{\varepsilon}_{kk})^2\, dv \qquad [1]$$

where $\int E(\dot{\varepsilon}^*)\, dv$ = work function = $\int \bar{\sigma} \cdot d\bar{\dot{\varepsilon}}$
$\int \mathbf{F} \cdot \mathbf{V}^* \cdot ds$ = boundary function which takes into account the frictional force (F) and admissible velocity V*
K = large positive constant which penalizes the dilational strain
$\dot{\varepsilon}_{kk}$ = strain-rate component
$\bar{\sigma}$ = effective stress = flow stress
$\bar{\dot{\varepsilon}}$ = effective strain rate

The work function takes into account in an *implicit* fashion the metallurgical phenomena which occur during hot working. For a given set of constitutive equations used in the work function, the numerical method offers an admissible solution to a given plasticity problem. It is often desirable to arrive at a unique or optimum solution, and this is possible only if the dynamic material behavior is incorporated *explicitly* into the finite-element method. The interconnective material constraints, however, are too complicated to be written directly in algebraic form. The development of a processing map[6,7] delineating the "safe" temperature–strain rate regimes for processing represents a major step toward acceptable solutions. Often, the "safe" regime defined by these maps is still a wide area[7] which provides several combinations of temperature and strain rate at which processing can be carried out. In this paper a method of modeling the dynamic material behavior in terms of a parameter which defines unique T-$\dot{\varepsilon}$ combination(s) for hot forming is presented and applied to the hot upsetting of Ti-6Al-2Sn-4Zr-2Mo-0.1Si (Ti-6242) alloy—a material of interest in the dual-property disk application.[8] The hot-deformation characteristics of this alloy in relation to the microstructure[3,9–11] have been studied earlier.

II. MODELING OF DYNAMIC MATERIAL BEHAVIOR

The basis for the modeling of dynamic material behavior is the unifying theme for the modeling of physical systems

Y. V. R. K. PRASAD, Associate Professor, Department of Metallurgy, Indian Institute of Science, Bangalore 560012, India, is now NRC-AFSC Senior Research Associate in Air Force Wright Aeronautical Laboratories (AFWAL/MLLM), Wright-Patterson Air Force Base, OH 45433. H. L. GEGEL is Senior Scientist, AFWAL/MLLM, Wright-Patterson Air Force Base, OH 45433. J. C. MALAS, J. T. MORGAN, and K. A. LARK are Materials Research Engineers, AFWAL/MLLM, Wright-Patterson Air Force Base, OH 45433. S. M. DORAIVELU and D. R. BARKER are Visiting Scientists, Universal Energy Systems, Inc., Dayton, OH 45432.
Manuscript submitted October 24, 1983.

as developed by Wellstead;[12] here systems are viewed as energy manipulators. In the metal-processing system, certain elements are stores and sources of energy, while the workpiece is the basic device for dissipating energy. The constitutive equation for the workpiece material is an analytical relation describing the variation of flow stress with process variables, namely, temperature and strain rate. This equation is an intrinsic characteristic of the workpiece material and describes the manner in which the energy is converted at any instant into a form—usually thermal or microstructural—which is not recoverable by the system. Thus, hot working is modeled in terms of management of several irreversible thermodynamic processes which are controlled by the rate of energy input and subsequent dissipation of that energy by dynamic metallurgical processes.

A typical constitutive relation for a simple dissipator is schematically represented in Figure 1(a) in the form of the variation of flow stress (effort) with strain rate (flow) at constant temperature and strain. At any given strain rate, the power P (per unit volume) absorbed by the workpiece during plastic flow is given by

$$\sigma \cdot \dot{\varepsilon} = \int_0^{\dot{\varepsilon}} \sigma \cdot d\dot{\varepsilon} + \int_0^{\sigma} \dot{\varepsilon} \cdot d\sigma \qquad [2a]$$

or

$$P = G + J \qquad [2b]$$

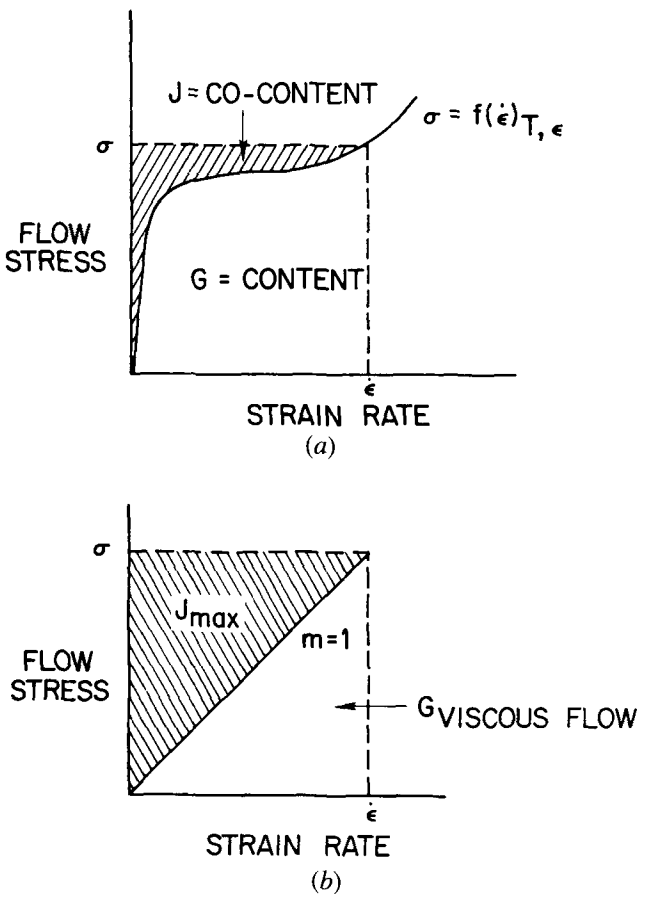

Fig. 1—(*a*) Schematic representation of G content and J co-content for workpiece having a constitutive equation represented by curve $\sigma = f(\dot{\varepsilon})$. Total power of dissipation is given by the rectangle. (*b*) Schematic representation showing J_{max} which occurs when strain-rate sensitivity (m) of material is equal to one.

In Figure 1(a) the area below the curve is $G = \int_0^{\dot{\varepsilon}} \sigma \cdot d\dot{\varepsilon}$, the dissipator content, and the area above the curve is $J = \int_0^{\sigma} \dot{\varepsilon} \cdot d\sigma$, the dissipator co-content. The G term represents the power dissipated by plastic work, most of which is converted into heat; the remaining small part is stored as lattice defects. The dissipator power co-content J is related to the metallurgical mechanisms which occur dynamically to dissipate power. The G content is the work function in Eq. [1], while the J co-content is a complementary set in the variational procedure. The dynamic material behavior can be modeled explicitly in terms of variations in the power co-content J with the process parameters.

Evaluation of Power Co-Content J

From Eq. [2a], it follows that at any given temperature and strain, the partitioning of power between J and G is given by:

$$\left(\frac{\partial J}{\partial G}\right)_{T,\varepsilon} = \left(\frac{\partial \ln \sigma}{\partial \ln \dot{\varepsilon}}\right)_{T,\varepsilon} \qquad [3]$$

which is merely the strain-rate sensitivity of the material conventionally evaluated as:

$$m = \left(\frac{\partial \ln \sigma}{\partial \ln \dot{\varepsilon}}\right)_{T,\varepsilon} \simeq \left(\frac{\Delta \log \sigma}{\Delta \log \dot{\varepsilon}}\right)_{T,\varepsilon} \qquad [4]$$

From Eq. [4] it also follows that the dynamic constitutive equation is of the type:

$$\sigma = A \cdot \dot{\varepsilon}^m \qquad [5]$$

In the hot-working range for pure metals,[2] m is temperature- and strain-rate independent; but in complicated alloy systems, it has been shown[3] to vary with temperature and strain rate.

At any given deformation temperature, J is evaluated by integrating Eq. [5] and, when combined with Eq. [5],

$$J = \int_0^{\sigma} \dot{\varepsilon} \cdot d\sigma = \frac{\sigma \cdot \dot{\varepsilon} \cdot m}{m + 1} \qquad [6]$$

From Eq. [6] the value of J at a given temperature and strain rate may be estimated from the flow stress and the strain-rate-sensitivity factor m. The value of J reaches its maximum (J_{max}) when $m = 1$, and the workpiece acts as a linear dissipator; thus,

$$J_{max} = \frac{\sigma \cdot \dot{\varepsilon}}{2} \qquad [7]$$

In this case, one-half of the power is dissipated as material flow and the other half is dissipated as heat [schematically shown in Figure 1(b)]. The behavior of superplastic materials approaches this extreme. The other extreme occurs for materials which are strain-rate insensitive and those which do not flow. In these cases J is zero.

The analogy for the above behavior is found in electrical systems where J_{max} corresponds to good electrical conductors and $J = 0$ corresponds to insulators. Common engineering materials processed at high temperatures exhibit flow behavior which falls somewhere between these two extremes. These materials are analogous to resistors in electrical systems, and their flow behavior under dynamic conditions may be characterized in terms of the J co-content.

For a given power input to the system, the material flow will be maximum when the workpiece dissipates the highest possible power through dynamic metallurgical processes, *i.e.*, the J co-content reaches its highest value.

The effect of J on the plastic flow of materials can be visualized if the power-dissipation capacity of the workpiece is expressed in terms of efficiency of dissipation, η, which is defined as the ratio of J to J_{max}. From Eqs. [6] and [7], it follows that

$$\eta = \frac{J}{J_{max}} = \frac{2m}{m + 1} \quad [8]$$

In simple terms the efficiency represents the dissipating ability of the workpiece as normalized with respect to the total power input to the system.

Several dynamic metallurgical processes contribute to power dissipation during hot working of materials, and these processes have characteristic ranges of efficiencies of dissipation. Often in materials having complicated microstructures or in two-phase alloys, these processes occur simultaneously and/or interactively. Thus, the evaluated value of J will be the overall result of these interactions. Metallurgical processes such as dynamic recovery, dynamic recrystallization, internal fracture (void formation or wedge cracking), dissolution or growth of particles or phases under dynamic conditions, dynamic spheroidization of acicular structures, and deformation-induced phase transformation or precipitation under dynamic conditions contribute to the changes in the dissipated power co-content J. When two major dissipation processes having different characteristics occur simultaneously, the value of J will reach its maximum when the energy of dissipation of one process equals that of the other. This is somewhat analogous to what happens in electrical systems[13] having a variable resistor where the load power reaches a maximum when the line and load resistances are equal. For processing of materials the most favorable conditions are those which provide the highest J dissipated in the most efficient fashion (highest η) and lie within the "safe" regions.

The power co-content J serves as the most useful index for characterizing dynamic material behavior in processing for the following reasons:

1. It defines unique combinations of T and $\dot{\varepsilon}$ for processing (peak values of J and η) and also separates the regimes which produce internal fracture.
2. Being a power term, it is an invariant and, hence, applicable to any state of stress.
3. It can be used conveniently as a non-holonomic constraint in the finite-element method.
4. It is a continuum parameter and can be integrated with the finite-element analysis.
5. In its estimation no specific atomistic rate-controlling mechanisms need be evaluated or assumed, although its variation with temperature and strain rate reflects the dominating dissipating mechanism. This aspect is advantageous, particularly when more than one mechanism is operating during hot forming.
6. From it, an algorithm can be developed which can be incorporated into process control.

III. MODELING OF HOT DEFORMATION OF Ti-6242

Ti-6242 is a near-α, $\alpha + \beta$ titanium alloy whose hot-working characteristics are very sensitive to the initial preform microstructure and processing variables. A processing technique is presently being developed for producing a dual-property turbine disk using these characteristics to synthesize microstructures which result in good tensile and low-cycle-fatigue properties in the bore region and good creep and stress-rupture properties in the rim region. For evaluating the constitutive behavior of this material, two different preform microstructures have been investigated:[3] equiaxed $\alpha + \beta$ and acicular $\alpha + \beta$ or transformed β. The first is an equilibrium microstructure of globular α in a matrix of transformed β (referred to as $\alpha + \beta$), while the second corresponds to a non-equilibrium transformed-β microstructure showing acicular α in the β matrix (referred to as β microstructure hereafter). Dadras and Thomas[3] have evaluated the relationship between the flow stress (σ), temperature (T), strain rate ($\dot{\varepsilon}$), and strain (ε) for these two starting preform microstructures using a hot-compression test. At small strain (0.04) the dependence of log σ upon $(1/T)$ was linear for the $\alpha + \beta$ preform, while dual-mode or bilinear behavior was reported for the β microstructure which exhibits a transition at about 930 °C (1203 K). The strain-rate sensitivities as obtained by the stress-relaxation technique were dependent upon strain rate and temperature for both preform microstructures.[3] These results suggest that the thermally activated behavior of this material is complicated and cannot be characterized by the apparent activation energy using conventional activation analysis of the hot-deformation process. In the following discussion, the constitutive behavior of Ti-6242 has been analyzed on the basis of the dynamic modeling method outlined earlier, and microstructural correlations have been attempted.

A. *Hot Deformation of the $\alpha + \beta$ Preform*

Variation of the flow stress with strain rate and temperature for the $\alpha + \beta$ microstructure is shown in Figures 2(a) and 2(b), corresponding to strains of 0.04 and 0.6, respectively. Data reported by Dadras and Thomas[3] (in the strain-rate range 10^{-3} to 10^{-1} s^{-1}) and Lewis[14] (1 s^{-1}) are represented in this plot. At each test temperature and strain rate, the strain-rate sensitivity m (Eq. [4]) is evaluated by fitting a polynomial equation to log σ-*vs*-log $\dot{\varepsilon}$ curves and obtaining the derivatives. The m values thus obtained are shown in Figures 3(a) and 3(b) as a function of temperature and strain rate for strains of 0.04 and 0.6, respectively. The instantaneous power dissipated by the material, the J co-content, at different temperatures and strain rates of deformation is estimated using Eq. [6] and is shown in Figure 4. The J value decreased gradually with increasing temperature and is higher at higher strain rates. A diffused peak is discernible at high rates. The efficiency of dissipation defined by Eq. [8] is also evaluated and plotted as a function of temperature at different strain rates in Figures 5(a) and 6. Some important features of these plots are:

1. The efficiency of power dissipation is higher at lower strain rates.

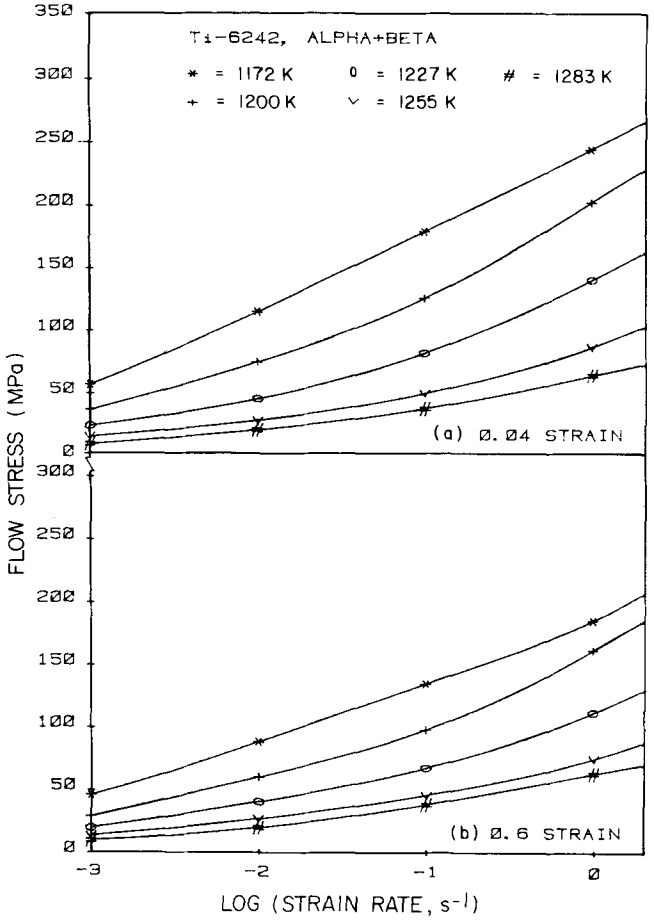

Fig. 2—Variation of flow stress with strain rate at different temperatures for Ti-6242 $\alpha + \beta$ preform (*a*) 0.04 strain and (*b*) 0.6 strain.

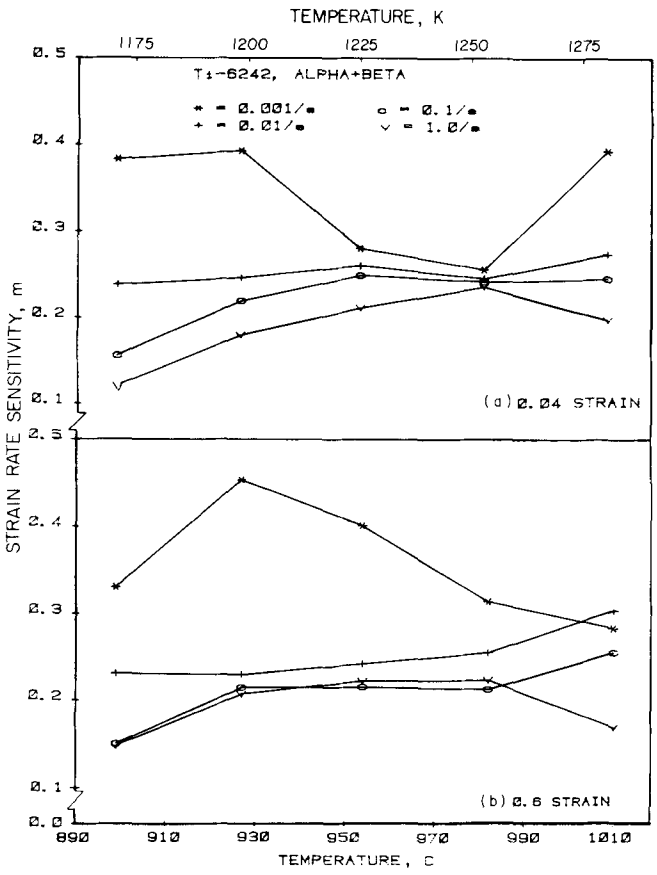

Fig. 3—Variation of strain-rate sensitivity (m) with temperature at different strain rates in Ti-6242 $\alpha + \beta$ preform (*a*) 0.04 strain and (*b*) 0.6 strain.

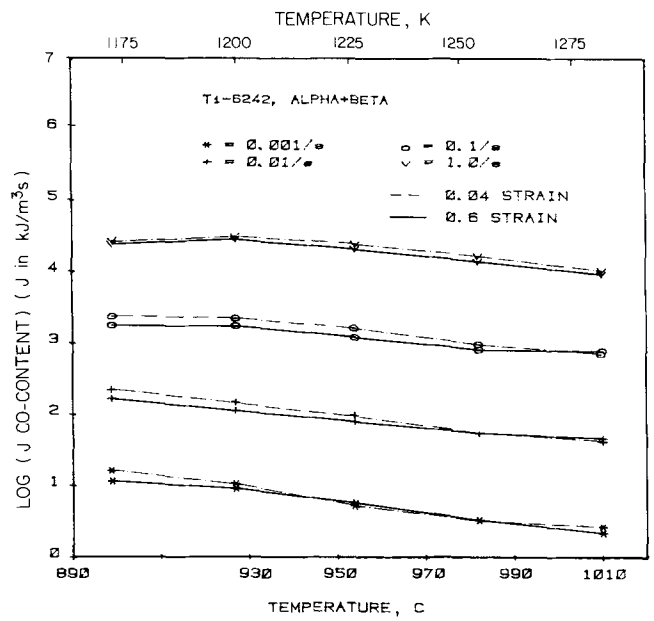

Fig. 4—Variation of J co-content with temperature at different strain rates in Ti-6242 $\alpha + \beta$ preform. Effect of strain is not significant.

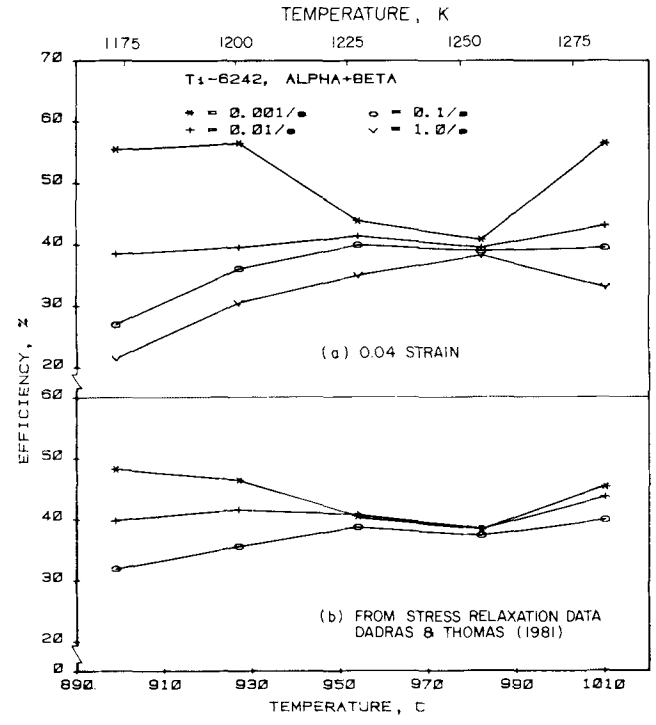

Fig. 5—(*a*) Variation of efficiency of dissipation with forging temperature for Ti-6242 $\alpha + \beta$ preform at a strain of 0.04 for different strain rates. (*b*) Efficiency of dissipation calculated from m obtained by stress-relaxation technique (Dadras and Thomas[3]).

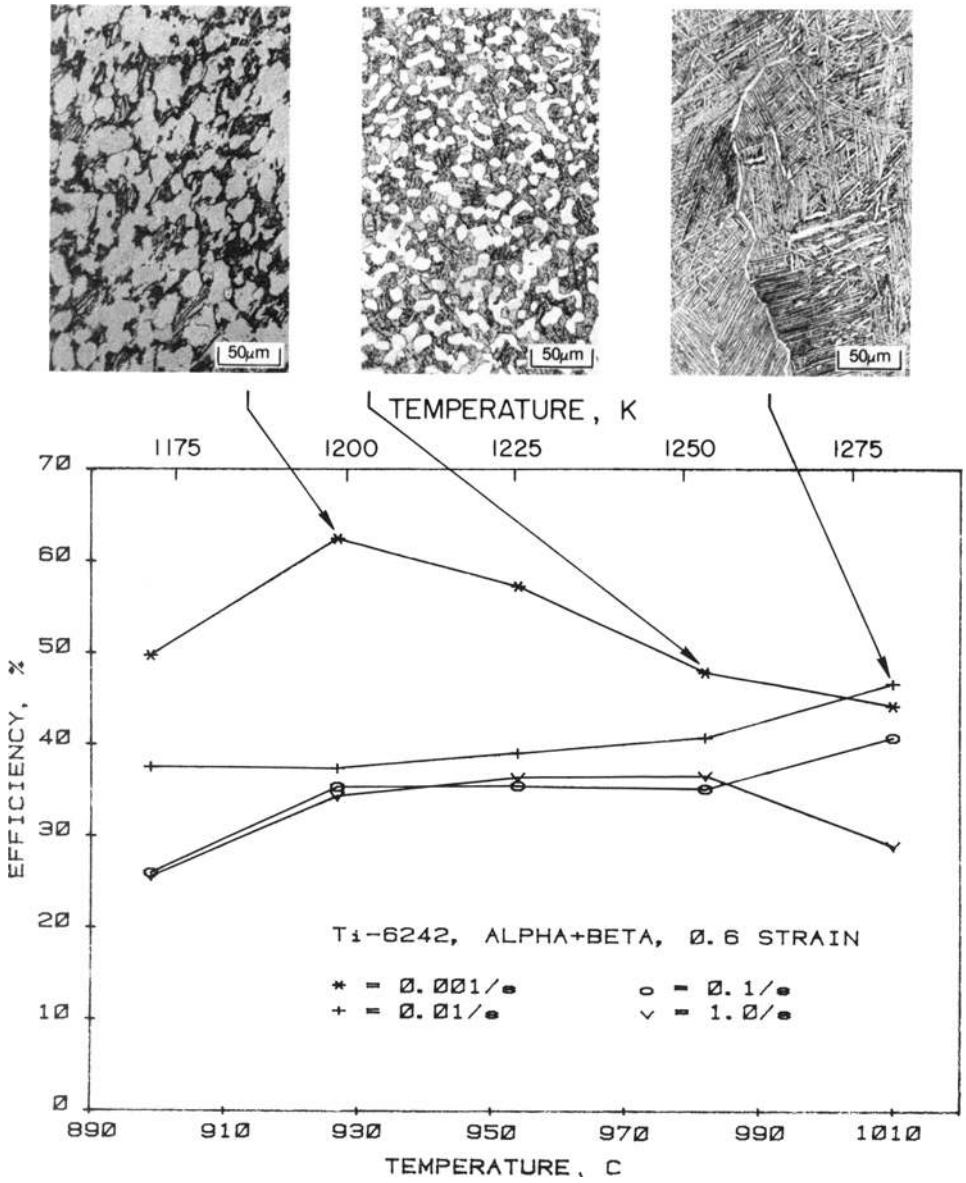

Fig. 6 — Variation of efficiency of dissipation through metallurgical processes with forging temperature for Ti-6242 $\alpha + \beta$ preform at a strain of 0.6 for different strain rates. Typical microstructures corresponding to particular processing temperatures and strain rates are also shown.

2. At each strain rate, the efficiency of power dissipation passes through a peak in the temperature range 899 to 982 °C (1172 to 1255 K).
3. At 982 °C (1255 K) the efficiency of dissipation obtained at all strain rates converges.
4. At 1010 °C (1283 K) the efficiency of dissipation is again strain-rate dependent, being higher at lower strain rates.
5. The features described above are essentially unchanged when the strain is increased from 0.04 to 0.6, as is evident from a comparison of Figures 5(a) and 6.

The efficiency of dissipation calculated from the m values obtained by Dadras and Thomas[3] from the stress-relaxation technique is shown in Figure 5(b) as a function of temperature at different strain rates. These variations are in good agreement with those given by Figure 5(a), although small differences in the magnitudes of the individual values exist.

In the temperature range 899 to 982 °C (1172 to 1255 K) ($\alpha + \beta$ field), the processing is best carried out at 927 °C (1200 K) and 10^{-3} s^{-1}, where the efficiency reaches its peak value (Figures 5 and 6). As the strain rate is increased, the efficiency of dissipation decreases and a wider range of temperature exists for processing, the minimum temperature being 927 °C (1200 K). The J variation with temperature (Figure 4) shows diffused peaks at 927 °C (1200 K) for strain rates of 0.1 and 1 s^{-1}; hence, a temperature of 927 °C (1200 K) is preferable for processing even at these strain rates.

The variation of efficiency of dissipation with temperature and strain rate is shown in the form of a three-dimensional map in Figure 7. The surface represented by these variations, although a complex one, highlights the regimes of processing which correspond to a high efficiency of dissipation. Another method of representing these results is shown in Figure 8 which is a contour map of constant

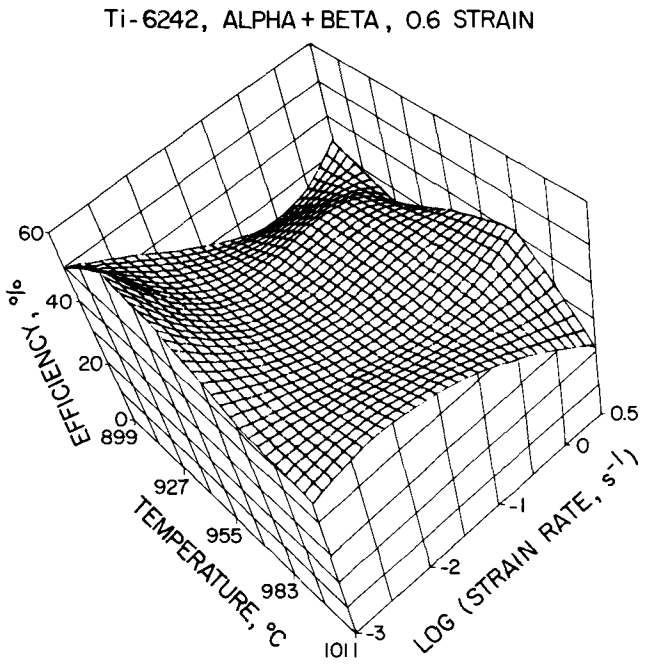

Fig. 7—Three-dimensional plot showing the variation of efficiency of dissipation with temperature and strain rate for Ti-6242 $\alpha + \beta$ preform at 0.6 strain.

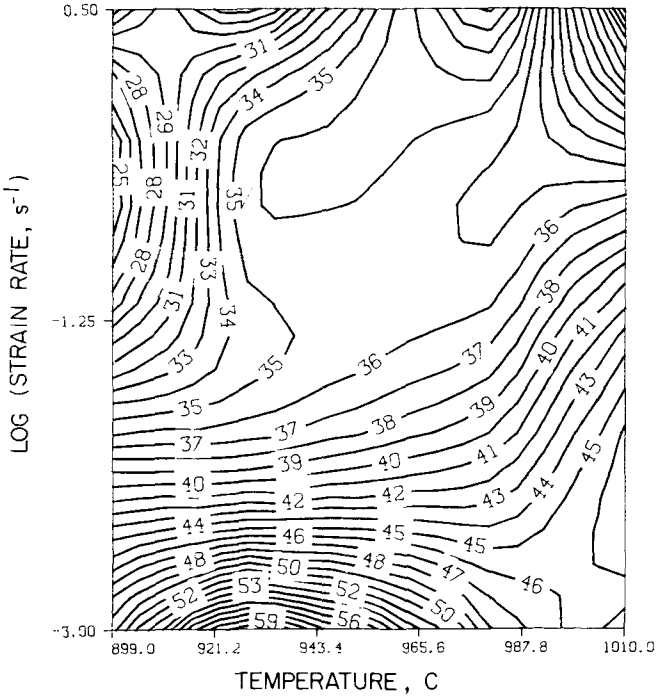

Fig. 8—Map showing constant efficiency contours in strain rate–temperature frame for Ti-6242 $\alpha + \beta$ preform at 0.6 strain.

efficiencies. The contour map is a two-dimensional representation of Figure 7 and is another convenient way to locate the processing regimes. For example, the optimum processing conditions of 927 °C (1200 K) and 10^{-3} s^{-1} are striking in Figure 8.

The metallurgical processes which are responsible for the observed variations may be identified by examining the microstructures. Typical microstructures recorded on Ti-6242 $\alpha + \beta$ material under different temperature and strain-rate conditions are shown in Figure 6, with a view toward correlation with the efficiency variations.

It is known that the β-transus for this material is at about 990 °C (1263 K); near this temperature, power dissipation occurs essentially by the phase transformation $\alpha + \beta \rightarrow \beta$. This phase transformation produces contraction[11] and its strain-rate dependence is not very significant, as evident from quantitative metallographic observations,[9] which show that the volume percent of primary α at 982 °C (1255 K) is nearly the same in specimens deformed at different strain rates. This accounts for the converging trend of dissipation curves for different strain rates at 982 °C (1255 K). Careful microstructural examination of the material deformed at 927 °C (1200 K) and 10^{-3} s^{-1} revealed recrystallization of the globular-α phase in the $\alpha + \beta$ microstructure (Figure 6). Furthermore, it has been shown by Semiatin, *et al.*,[9] that the primary-α content in the microstructure decreases with increasing temperature, *i.e.*, $\alpha + \beta \rightarrow \beta$ transformation occurs to a greater extent. Thus, at least two important power-dissipation processes occur during hot deformation of $\alpha + \beta$ preforms—dynamic recrystallization and $\alpha + \beta \rightarrow \beta$ phase transformation. The peak in the efficiency-temperature curve represents the temperature at which the power of dissipation (rate of energy dissipation) due to dynamic recrystallization is equal to that due to phase transformation. On the left of the peak, dynamic recrystallization dominates while on the right, phase transformation is dominant. The peak is diffused over a wider temperature range when these two processes balance their rates of energy dissipation over this range.

At 1010 °C (1283 K) the material is deforming as a β phase, and the grain size is large (250 to 350 μm).[3,9] There is no evidence of dynamic recrystallization. On the other hand, grain-boundary sliding is a possibility at lower strain rates and causes wedge cracking which could, in turn, also dissipate energy with high efficiency. Dissipation by this mechanism is reduced at higher strain rates since grain-boundary sliding is less; the data in Figure 5(a) support this. At higher strain rates, dissipation can occur by dynamic recovery processes. Metallographic examination of specimens deformed at 1010 °C (1283 K) and at low strain rates revealed the transformed-α phase in the wedge-crack or intergranular-crack morphology. This phase occurs because the specimens undergo a non-equilibrium phase transformation when air cooled; for the thermodynamic reasons outlined earlier,[11] the transformed-α preferentially forms at sites of high tensile–hydrostatic stress.

B. *Hot Deformation of the β Preform*

Analysis similar to that described above for $\alpha + \beta$ preform materials has been carried out on β-preform material also. The variations of the J co-content with test temperature for different strain rates is shown in Figure 9 for strains of 0.04 and 0.6. These plots are very similar to those obtained on the $\alpha + \beta$ preform (Figure 4). The efficiency of dissipation (Eq. [8]) is plotted as a function of temperature for different strain rates in Figure 10. These variations are considerably different from those obtained on the $\alpha + \beta$ preform (Figures 5 and 6). Referring to Figure 10(a) (strain of 0.04), when the material is deformed at 10^{-3} s^{-1}, a drop in the efficiency of dissipation is evident at temperatures higher than 954 °C (1227 K). At higher strain rates

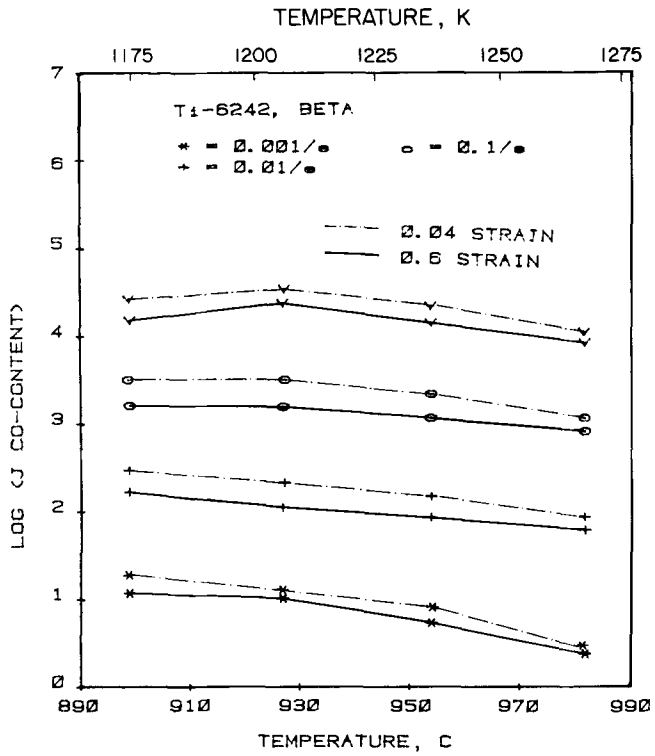

Fig. 9—Variation of J co-content with temperature for different strain rates in Ti-6242 β-preform. Effect of strain is also shown.

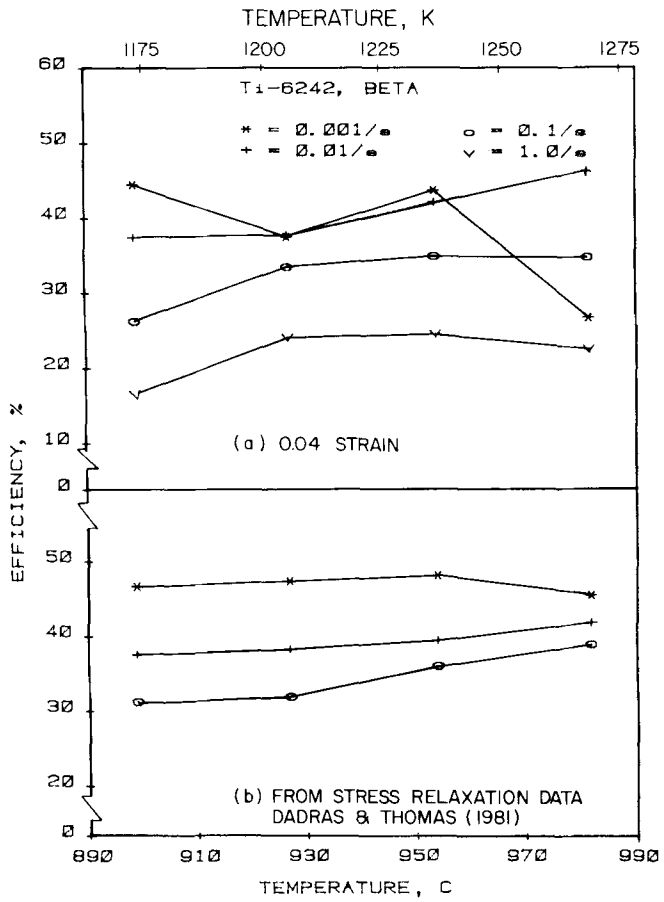

Fig. 10—(*a*) Variation of efficiency of dissipation with temperature of forging for β-preform of Ti-6242 at a strain of 0.04 for different strain rates. (*b*) Efficiency of dissipation calculated from m obtained by stress-relaxation technique (Dadras and Thomas[3]).

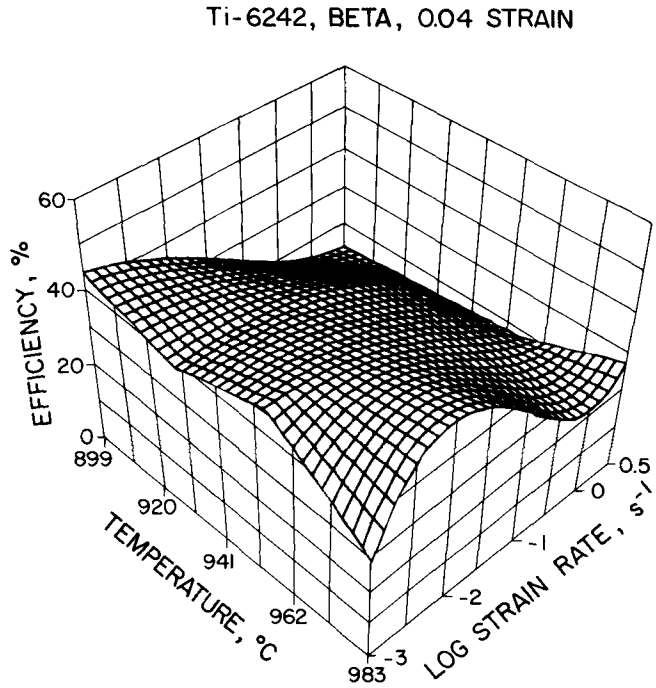

Fig. 11—Three-dimensional plot showing variation of efficiency of dissipation with temperature and strain rate for Ti-6242 β-preform at 0.04 strain.

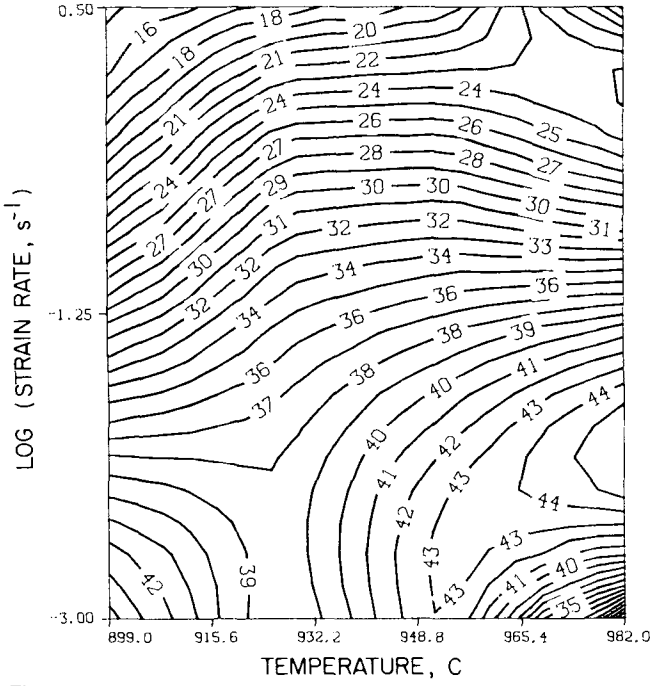

Fig. 12—Map showing constant efficiency contours in strain rate–temperature frame for Ti-6242 β-preform at 0.04 strain.

(10^{-1} and 1 s^{-1}), a diffused efficiency peak occurs between 927 °C (1200 K) and 954 °C (1227 K). At 10^{-2} s^{-1}, however, the efficiency of dissipation increases with an increase in temperature beyond 927 °C (1200 K). Figure 10(b) shows the efficiency of dissipation calculated from the strain-rate sensitivity measured using the stress-relaxation technique.[3] Except for the value at 927 °C (1200 K) and 10^{-1} s^{-1}, the data show trends similar to those in Figure 10(a). The three-dimensional efficiency-temperature-strain rate map and the corresponding contour map for

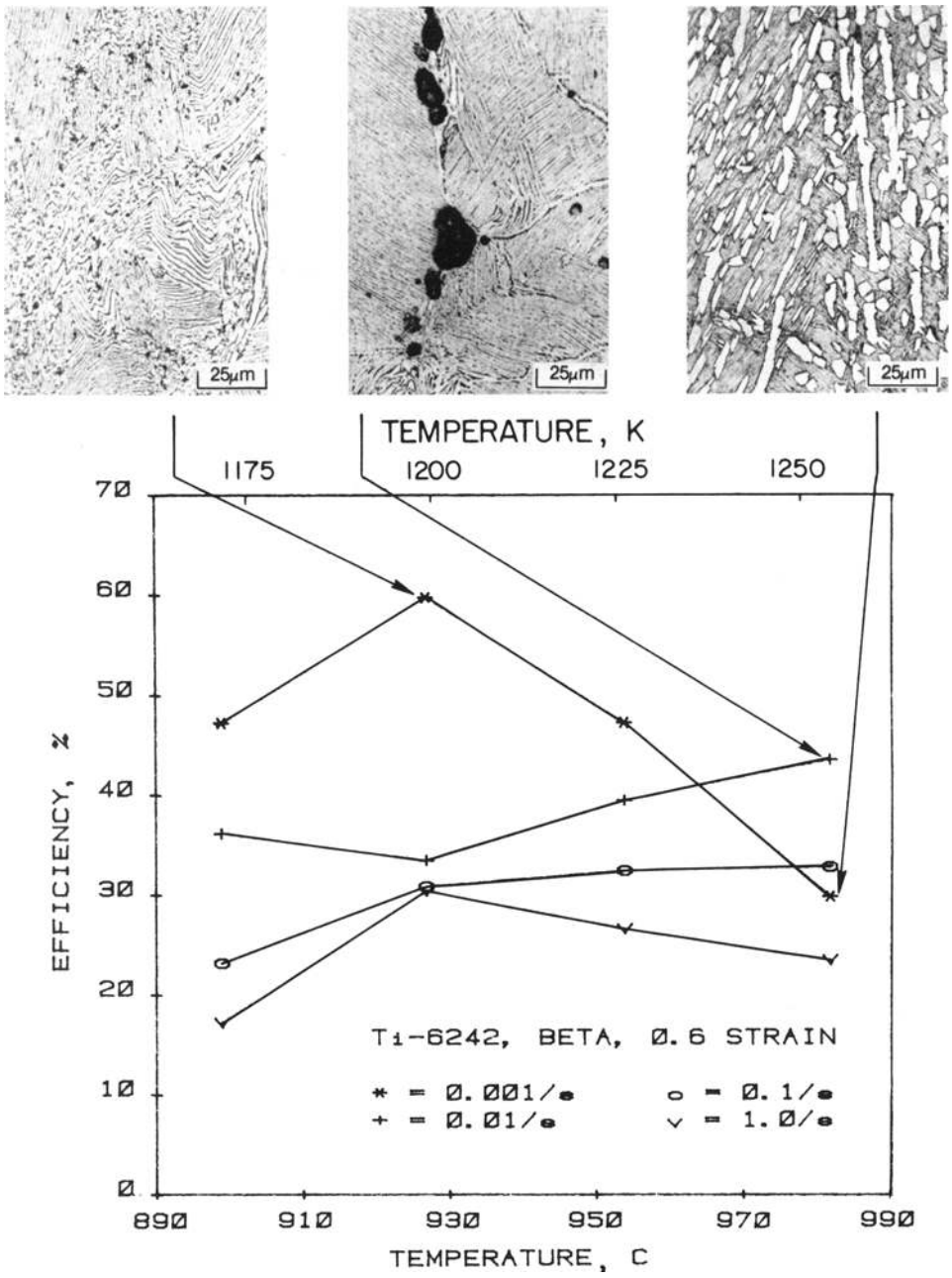

Fig. 13 — Variation of efficiency of dissipation through metallurgical processes with forging temperature for Ti-6242 β-preform at a strain of 0.6 for different strain rates. Typical microstructures corresponding to particular processing temperatures and strain rates are also shown.

the β-Ti-6242 at a strain of 0.04 are shown in Figures 11 and 12, respectively. The drop in the efficiency of dissipation at 982 °C (1255 K) and $10^{-3}\,s^{-1}$ is clearly revealed in these maps.

For a strain of 0.6, the efficiency variations are shown in Figure 13 and the corresponding three-dimensional maps and efficiency contours are shown in Figures 14 and 15, respectively. These figures show that two well-defined peaks occur in the temperature-strain rate regime — one at 927 °C (1200 K) and $10^{-3}\,s^{-1}$ and the other at 927 °C (1200 K) and $1\,s^{-1}$. The behavior at strain rates of 10^{-2} and $10^{-1}\,s^{-1}$ remains the same as for low strains. The data clearly show that optimum forging conditions for the β-preform are 927 °C (1200 K) and $10^{-3}\,s^{-1}$; and if the forging is carried out at high strain rates ($1\,s^{-1}$), the best temperature would still be 927 °C (1200 K).

Correlation between efficiency variations and metallurgical changes is provided in Figure 13. The microstructures in Figure 13 reflect the metastable nature of the β-preform which shows a tendency toward a more stable microstructural form — the $\alpha + \beta$ structure. From the metallographic evidence available, the large drop in efficiency at $10^{-3}\,s^{-1}$ and temperatures beyond 927 °C (1200 K) (Figure 13) is associated with the precipitation

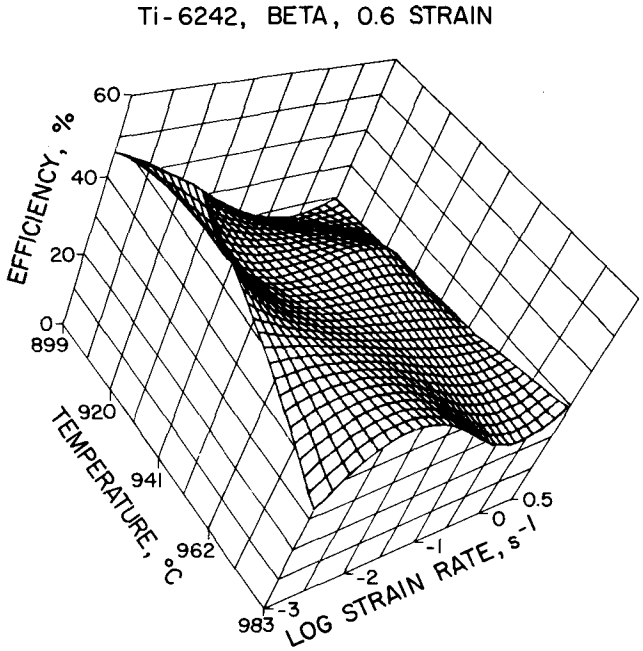

Fig. 14—Three-dimensional plot showing variation of efficiency of dissipation with temperature and strain rate for Ti-6242 β-preform at 0.6 strain.

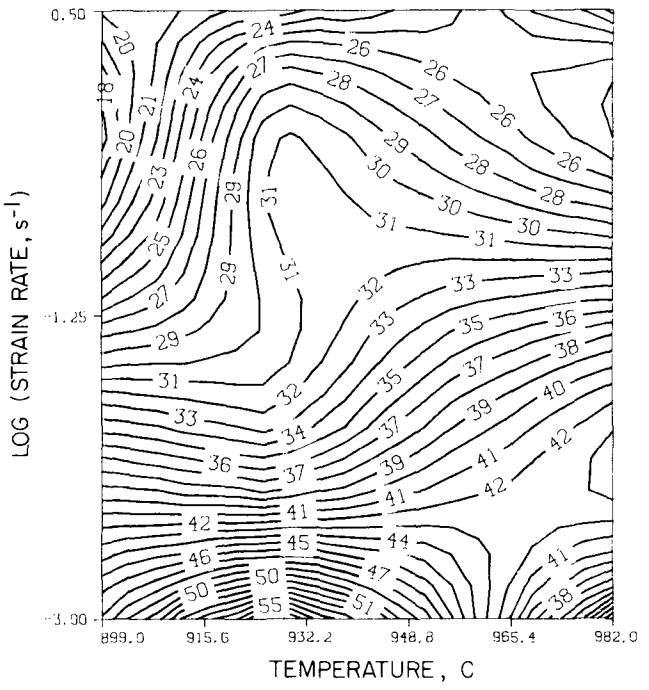

Fig. 15—Map showing constant efficiency contours in strain rate–temperature frame for Ti-6242 β-preform at 0.6 strain.

of transformed-α from the metastable-β structure.[3,9] At lower strains this precipitation occurs at higher temperatures (>954 °C or 1227 K) (Figure 9(a)). At lower strain rates ($\leq 10^{-2}$ s^{-1}), some grain-boundary sliding also occurs, resulting in wedge cracks and grain-boundary cavities[11,15,16] which aid in energy dissipation. Thus, the two opposing dissipation processes are (1) the precipitation of transformed-α (which reduces the rate of energy dissipation) and (2) wedge cracking and grain-boundary cavitation (which increase the rate of energy dissipation). At high strain rates (~ 1 s^{-1}), grain-boundary sliding is minimal while at 10^{-3} s^{-1}, the precipitation of transformed-α is more dominant than grain-boundary sliding. It is interesting to note that the transformed-α occurs at wedge cracks and grain-boundary cavities,[11] and this is a dynamic process in view of the metastable nature of the β-preform microstructure. At 10^{-2} s^{-1}, wedge cracking dominates[16] at temperatures above 927 °C (1200 K) and, hence, the efficiency of dissipation increases with an increase in temperature. At 899 °C (1172 K) the dissipation processes involved are local kinking of β-platelets and spheroidization, the former dominating at higher strain rates (~ 1 s^{-1}) and the latter at lower strain rates ($\sim 10^{-3}$ s^{-1}).

IV. SUMMARY

A method of modeling material behavior which explicitly describes the dynamic metallurgical processes occurring during hot deformation has been presented. Following a systems approach, metal processing is considered as a system in which the workpiece material is a dissipator of power. The dissipated power co-content, J, represents the dynamic metallurgical processes occurring during hot working while its complementary part, the G content, represents the power dissipation through heat. The partitioning of power between J and G is controlled by strain-rate sensitivity, m. It is shown that J is related to m and reaches a maximum value (J_{max}) when $m = 1$. The efficiency of dissipation (J/J_{max}) is a characteristic of the metallurgical process responsible for the dissipation and can lead to a unique combination of temperature and strain rate for processing and also delineate regions of internal fracture. This method of modeling is effective even when several metallurgical processes occur simultaneously during hot deformation, since no prior knowledge or evaluation of the atomistic mechanisms is required.

The above method has been validated by modeling Ti-6242 material during hot forging. The analysis revealed that the optimum forging condition for forging both $\alpha + \beta$ and β-preform microstructures is obtained at 927 °C (1200 K) and 10^{-3} s^{-1}. A good correlation between the efficiency variations and microstructural changes occurring during hot deformation could be established in this material. For the $\alpha + \beta$ preform, dynamic recrystallization and phase transformation are important in the temperature range 899 to 982 °C (1172 to 1255 K), while at 1010 °C (1283 K) dissipation at low strain rates occurs by wedge cracking. Regarding the β-preform, local kinking of β-platelets, spheroidization of the acicular structure, precipitation of transformed-α, and wedge cracking have been shown to influence the efficiency of dissipation.

ACKNOWLEDGMENTS

Dr. Prasad expresses his gratitude to the National Research Council, Washington, DC, for awarding the NRC-AFSC Research Associateship and to the Indian Institute of Science, Bangalore, for granting a sabbatical leave to conduct research at Wright-Patterson Air Force Base. The authors wish to thank Professors J. F. Thomas, Jr. and

P. Dadras of Wright State University and Dr. S. L. Semiatin of Battelle Columbus Laboratories for helpful discussions. Thanks are also due to Mrs. M. Whitaker and Mrs. H. L. Henrich (Systems Research Laboratories, Inc.) for editorial assistance and preparation of the manuscript.

REFERENCES

1. H. J. McQueen and J. J. Jonas: *Metal Forming—Interrrelation between Theory and Practice*, A. L. Hoffmanner, ed., Plenum Press, New York, NY, 1971, p. 393.
2. J. J. Jonas, C. M. Sellars, and W. J. McG.Tegart: *Met. Rev.*, 1969, vol. 14, p. 1.
3. P. Dadras and J. F. Thomas, Jr.: *Metall. Trans. A*, 1981, vol. 12, p. 1867.
4. C. H. Lee and S. Kobayashi: *Trans. ASME, J. Engr. Ind.*, 1973, vol. 95, p. 865.
5. S. I. Oh: *Int. J. Mech. Sci.*, 1982, vol. 24, p. 479.
6. R. Raj: *Metall. Trans. A*, 1981, vol. 12, p. 1089.
7. K. P. Rao, S. M. Doraivelu, H. Md. Roshan, and Y. V. R. K. Prasad: *Metall. Trans. A*, 1983, vol. 14, p. 1671.
8. G. D. Lahoti, S. L. Semiatin, S. I. Oh, T. Altan, and H. L. Gegel: *Advanced Processing Methods for Titanium*, D. F. Hasson and C. H. Hamilton, eds., TMS-AIME, Warrendale, PA, 1981, p. 23.
9. S. L. Semiatin, J. F. Thomas, Jr., and P. Dadras: *Metall. Trans. A*, 1983, vol. 14, p. 2363.
10. S. L. Semiatin and G. D. Lahoti: *Metall. Trans. A*, 1981, vol. 12, p. 1705.
11. H. L. Gegel: *Proceedings of Symposium on Experimental Verification of Process Models*, 1981, Metals Congress, September 21-23, 1981, Cincinnati, OH, C. C. Chen, ed., ASM, Metals Park, OH, 1983, p. 32.
12. P. E. Wellstead: *Introduction to Physical System Modeling*, Academic Press, New York, NY, 1979, pp. 9, 144.
13. C. S. Siskind: *Electrical Circuits*, McGraw-Hill Book Co., New York, NY, 1965, p. 565.
14. G. K. Lewis: AFWAL-TR-80-4162, AFWAL Materials Laboratory, Wright-Patterson Air Force Base, OH 45433, 1980.
15. H. L. Gegel, S. Nadiv, and R. Raj: *Scripta Met.*, 1980, vol. 14, p. 241.
16. J. C. Malas, H. L. Gegel, S. I. Oh, and G. D. Lahoti: *Proceedings of Symposium on Experimental Verification of Process Models*, 1981 Metals Congress, September 21-23, 1981, Cincinnati, OH, C. C. Chen, ed., ASM, Metals Park, OH, 1983, p. 358.